



**HAL**  
open science

## Evaluation of an improved intermediate complexity snow scheme in the ORCHIDEE land surface model

Tao Wang, Catherine Ottle, Aaron Anthony Boone, Philippe Ciais, Eric Brun, Samuel Morin, Gerhard Krinner, Shilong Piao, Shushi Peng

### ► To cite this version:

Tao Wang, Catherine Ottle, Aaron Anthony Boone, Philippe Ciais, Eric Brun, et al.. Evaluation of an improved intermediate complexity snow scheme in the ORCHIDEE land surface model. *Journal of Geophysical Research: Atmospheres*, 2013, 118 (12), pp.6064-6079. 10.1002/jgrd.50395 . hal-02930046

**HAL Id: hal-02930046**

**<https://hal.science/hal-02930046>**

Submitted on 28 Oct 2020

**HAL** is a multi-disciplinary open access archive for the deposit and dissemination of scientific research documents, whether they are published or not. The documents may come from teaching and research institutions in France or abroad, or from public or private research centers.

L'archive ouverte pluridisciplinaire **HAL**, est destinée au dépôt et à la diffusion de documents scientifiques de niveau recherche, publiés ou non, émanant des établissements d'enseignement et de recherche français ou étrangers, des laboratoires publics ou privés.

## Evaluation of an improved intermediate complexity snow scheme in the ORCHIDEE land surface model

Tao Wang,<sup>1,2</sup> Catherine Ottlé,<sup>1</sup> Aaron Boone,<sup>3</sup> Philippe Ciais,<sup>1</sup> Eric Brun,<sup>3</sup> Samuel Morin,<sup>4</sup> Gerhard Krinner,<sup>2</sup> Shilong Piao,<sup>5,6</sup> and Shushi Peng<sup>1,2</sup>

Received 4 December 2012; revised 2 April 2013; accepted 5 April 2013; published 20 June 2013.

[1] Snow plays an important role in land surface models (LSM) for climate and hydrometeorological studies, but its current treatment as a single layer of constant density and thermal conductivity in ORCHIDEE (Organizing Carbon and Hydrology in Dynamic Ecosystems) induces significant deficiencies. The intermediate complexity snow scheme ISBA-ES (Interaction between Soil, Biosphere and Atmosphere-Explicit Snow) that includes key snow processes has been adapted and implemented into ORCHIDEE, referred to here as ORCHIDEE-ES. In this study, the adapted scheme is evaluated against the observations from the alpine site Col de Porte (CDP) with a continuous 18 year data set and from sites distributed in northern Eurasia. At CDP, the comparisons of snow depth, snow water equivalent, surface temperature, snow albedo, and snowmelt runoff reveal that the improved scheme in ORCHIDEE is capable of simulating the internal snow processes better than the original one. Preliminary sensitivity tests indicate that snow albedo parameterization is the main cause for the large difference in snow-related variables but not for soil temperature simulated by the two models. The ability of the ORCHIDEE-ES to better simulate snow thermal conductivity mainly results in differences in soil temperatures. These are confirmed by performing sensitivity analysis of ORCHIDEE-ES parameters using the Morris method. These features can enable us to more realistically investigate interactions between snow and soil thermal regimes (and related soil carbon decomposition). When the two models are compared over sites located in northern Eurasia from 1979 to 1993, snow-related variables and 20 cm soil temperature are better reproduced by ORCHIDEE-ES than ORCHIDEE, revealing a more accurate representation of spatio-temporal variability.

**Citation:** Wang, T., C. Ottlé, A. Boone, P. Ciais, E. Brun, S. Morin, G. Krinner, S. Piao, and S. Peng (2013), Evaluation of an improved intermediate complexity snow scheme in the ORCHIDEE land surface model, *J. Geophys. Res. Atmos.*, 118, 6064–6079, doi:10.1002/jgrd.50395.

### 1. Introduction

[2] Snow covers nearly half of the Northern Hemisphere (NH) land surface in the cold season [Robinson *et al.*, 1993; Lemke *et al.*, 2007]. Because of its large seasonal

variability and distinct physical properties (i.e., high albedo, low thermal conductivity, and low roughness length), snow can exert strong positive feedbacks on local climate [Groisman *et al.*, 1994; Qu and Hall, 2006; Fernandes *et al.*, 2009; Flanner *et al.*, 2011]. Snow cover also influences atmospheric variability and seasonal climate predictability in the NH [Gong *et al.*, 2007; Fletcher *et al.*, 2009; Douville, 2010]. In addition, snow water storage impacts runoff, soil moisture, and evaporation [e.g., Groisman *et al.*, 2004]. For example, snow can act as a moisture reservoir in cold semiarid and arid regions, where vegetation activity is found to be related to spring snowmelt [e.g., Peng *et al.*, 2010, Tahir *et al.*, 2011].

[3] A variety of snow models have been developed, ranging from simple degree-day models [e.g., Hock, 2003], snow schemes of intermediate complexity [e.g., Boone and Etchevers, 2001; Shrestha *et al.*, 2010], to detailed snow-pack models [e.g., Brun *et al.*, 1992; Lehning *et al.*, 2002, Rasmus *et al.*, 2007]. By comparing the results of 1701 combinations of parameterizations currently used in intermediate complexity snow models at an alpine site, Essery *et al.*

<sup>1</sup>Laboratoire des Sciences du Climat et de l'Environnement, CEA CNRS UVSQ, Gif-sur-Yvette, France.

<sup>2</sup>Laboratoire de Glaciologie et Géophysique de l'Environnement, UMR5183, CNRS/, Université Joseph Fourier-Grenoble, Grenoble, France.

<sup>3</sup>CNRM-GAME, Météo-France and CNRS, Toulouse, France.

<sup>4</sup>CNRM-GAME, Météo-France and CNRS, Centre d'Études de la Neige, Grenoble, France.

<sup>5</sup>Sino-French Institute for Earth System Science, College of Urban and Environmental Sciences, Peking University, Beijing, China.

<sup>6</sup>Institute of Tibetan Plateau Research, Chinese Academy of Sciences, Beijing, China.

Corresponding author: Corresponding author: T. Wang, Laboratoire des Sciences du Climat et de l'Environnement, CEA CNRS UVSQ, 91191 Gif-sur-Yvette, France. (tao.wang@lscce.ipsl.fr)

[2013] showed that good performance always stems from model configurations that have prognostic representation of snow albedo and snow density and that account for storage and refreezing of liquid water within the snowpack. The importance of these processes in a snow model has also been emphasized in previous studies [e.g., Slater *et al.*, 2001; Rutter *et al.*, 2009]. For example, Rutter *et al.* [2009] showed that the representation of a vertically heterogeneous snowpack is very important since incomplete melting enables the presence of liquid water that is allowed for later freezing and can also significantly change snow pack properties. However, these important snow physical processes are not considered in the current snow module of the ORCHIDEE (Organizing Carbon and Hydrology in Dynamic Ecosystems) LSM, although this model has been used for hydrological applications [e.g., Piao *et al.*, 2007] and land-atmosphere coupling with LMDz (Laboratoire de Météorologie Dynamique zoom). Recently, Gouttevin *et al.* [2012a] reported that using spatially variable instead of constant values of the bulk snow effective thermal conductivity of the snowpack in different regions in ORCHIDEE would lead to a difference of 8% in simulated pan-arctic soil carbon stocks. This highlights that snow physical processes are critical for many processes operating in the underlying soil and that snow processes in ORCHIDEE should be better resolved to build confidence for accurate representation of snow characteristics in these high-latitude regions.

[4] Acknowledging the limitations of single-layer scheme [e.g., Dutra *et al.*, 2012], we introduce an intermediate complexity snow model largely inspired from ISBA-ES (Interaction between Soil, Biosphere and Atmosphere-Explicit Snow) [Boone and Etchevers, 2001] accounting for snow settling, water percolation, and refreezing into ORCHIDEE (called ORCHIDEE-ES hereafter). The main purpose of this study is to evaluate ORCHIDEE-ES against snow observations. Previous snow model evaluations have often been restricted to a few sites [e.g., Brown *et al.*, 2006; Shrestha *et al.*, 2010]. In snow model intercomparisons [e.g., Rutter *et al.*, 2009; Essery *et al.*, 2013], snow model performances were found to be variable across sites and years. It is thus necessary to develop snow model evaluations spanning across large spatial and temporal scales [e.g., Pan *et al.*, 2003; Habets *et al.*, 2008; Parajka *et al.*, 2010]. This becomes possible since numerous in situ snow data from surface observation networks can be accessed [e.g., Dyer and Mote, 2006; Parajka *et al.*, 2010; Peng *et al.*, 2010; Brun *et al.*, 2013]. In a multisite evaluation exercise, one limitation is the lack of collocated meteorological forcing used for driving models locally. This can be overcome by the use of state-of-the-art meteorological reanalyses, e.g., ERA-Interim reanalysis [Brun *et al.*, 2013]. In this study, snow in ORCHIDEE is thus evaluated at sites with meteorological variables either measured in situ or sampled from reanalysis products. Moreover, a global sensitivity analysis of ORCHIDEE-ES is performed on one site based on the Morris method [Morris, 1991] to characterize the relative influence of different related parameters when studying snow. The paper is organized as follows. Section 2 introduces the physical parameterizations used in the improved snow scheme. Section 3 describes the statistical metrics used for model evaluation. Section 4 describes the model evaluation and model sensitivity tests at the

experiment site Col de Porte. Section 5 provides the model evaluation results at sites covering large spatial and temporal scales in northern Eurasia.

## 2. Model Description

### 2.1. Representation of Snow Processes in the Current ORCHIDEE Version

[5] The snow module in the version 1.9.6 of ORCHIDEE is a simple scheme designed for use in general circulation models [Chalita and Le Treut, 1994], where snowpack processes are coarsely represented. Snow is described with a single bucket of constant snow density ( $330 \text{ kg m}^{-3}$ ). Snow surface temperature is derived by resolving energy budget equation taking into account incoming shortwave and longwave radiations, sensible and latent heat flux, and ground heat flux in the skin layer that is assumed to be an infinitesimal layer without heat capacity. When surface temperature is simulated to be above freezing, it is automatically reset to  $0^\circ\text{C}$  in the snow, and the excess energy is applied to melt snow. Snowmelt directly feeds runoff, since liquid water is not allowed to be stored in the snowpack. This simplification implies that ORCHIDEE is not capable to represent liquid water refreezing and the related heat release used to limit the cooling of the snow layer. In addition, a mixed snow-soil structure is assumed, which implies that temperature in the first soil layer is set equal to the snow temperature. The initial snow albedo values of bare soil and each plant functional type are prescribed, and their values are updated with both snow age and new snowfall. Snow albedo is then weighted by the fractional snow coverage over a grid cell leading to rapid variations of albedo during the ablation period when the snow fraction decreases [Chalita and Le Treut, 1994].

### 2.2. Representation of Snow Processes in ORCHIDEE-ES

#### 2.2.1. Snow Layering

[6] The ORCHIDEE LSM with the improved snow module referred to here as ORCHIDEE-ES is presented in details in the following. The structural differences between ORCHIDEE and ORCHIDEE-ES are shown in Figure 1. The snowpack in ORCHIDEE-ES is represented with three snow layers, which is shown to adequately resolve the snow thermal gradients between the top and base of the snow cover [Lynch-Stieglitz, 1994; Sun *et al.*, 1999]. In order to have a reasonable simulation of diurnal change in surface temperature, the maximum upper layer thickness is prescribed to be 5 cm ( $D_{j1\text{max}}$ ). In addition, since the diurnal variations of snowpack thermal properties are most pronounced near the snow surface, the thickness of the second layer is limited to 50 cm. The definition of snow layer thickness can be found as follows [Lynch-Stieglitz, 1994; Boone and Etchevers, 2001].

$$D_{j1} = \delta_D 0.25 D_j + (1 - \delta_D) D_{j1\text{max}} \quad (1)$$

$$D_{j2} = \delta_D 0.50 D_j + (1 - \delta_D) [0.34 (D_j - D_{j1\text{max}}) + D_{j1\text{max}}] (D_{j2} \leq 10 D_{j1}) \quad (2)$$

$$D_{j3} = D_j - D_{j1} - D_{j2} \quad (3)$$

$D_{j1}$ ,  $D_{j2}$ ,  $D_{j3}$ , and  $D_j$  are the first layer, second layer, third layer, and total snow thickness (cm).  $\delta_D$  is 0 and 1, respectively, when  $D_j$  is above and below 20 cm.

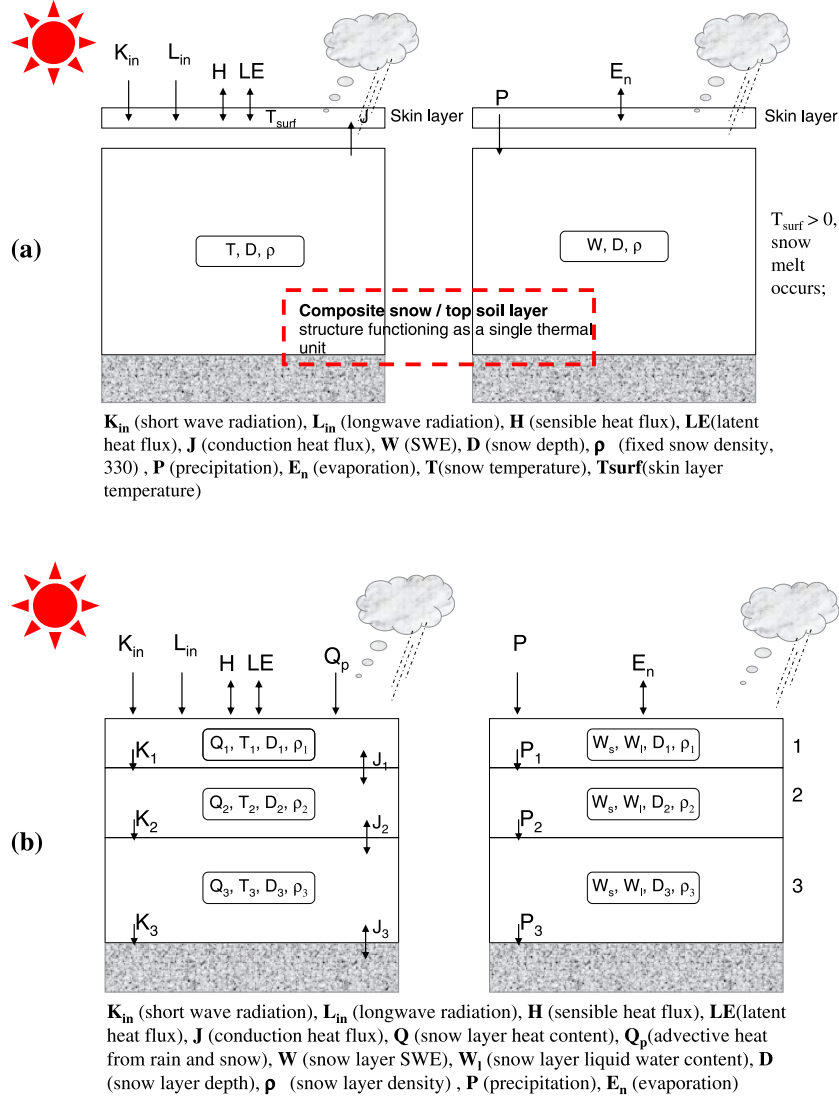


**Figure 1.** The soil module coupled with (a) a one-layer snow module in ORCHIDEE and (b) a three-layer snow module in ORCHIDEE-ES.

### 2.2.2. Energy Balance and Transfer

[7] In ORCHIDEE, vertical diffusion equations are used to describe heat conduction from the bottom of the soil to the skin layer, which is achieved by the implicit method through coupling one-layer snow bucket model and the thermodynamic soil model to the surface energy balance [Polcher *et al.*, 1998]. The same scheme is implemented in ORCHIDEE-ES but includes solar radiation absorption by each snow layer; the first snow layer instead of the skin layer as in ORCHIDEE is used to calculate the surface energy balance.

[8] At each half-hourly model time step, energy is transferred through the snow/soil column based on the vertical heat-transfer equation,

$$C_p \frac{\partial T_j}{\partial t} = \frac{\partial}{\partial z} \left( \kappa_j \frac{\partial T_j}{\partial z} \right) + \frac{\partial R}{\partial z} \quad (4)$$

where  $T_j$  is snow temperature,  $z$  is vertical coordinate,  $t$  is time, and  $C_p$  is snow or soil heat capacity ( $\text{J m}^{-3} \text{K}^{-1}$ ). Snow  $C_p$  is the product of snow density ( $\rho_i$ ,  $\text{kg m}^{-3}$ ) and specific

heat of ice ( $2106 \text{ J K}^{-1} \text{ kg}^{-1}$ ). Compared to the constant value used in ORCHIDEE, the thermal conductivity of the snow in ORCHIDEE-ES,  $k_j$  ( $\text{W m}^{-1} \text{K}^{-1}$ ) is given by

$$k_j = (a_\lambda + b_\lambda \rho_i^2) + \left( a_{\lambda v} + \frac{b_{\lambda v}}{T_j - c_{\lambda v}} \right) \left( \frac{P_0}{P_a} \right) \quad (5)$$

where the parameters  $a_\lambda = 0.02$ ,  $b_\lambda = 2.50 \times 10^{-6}$ ,  $a_{\lambda v} = -0.06$ ,  $b_{\lambda v} = -2.54$ ,  $c_{\lambda v} = -289.99$ , and  $P_a$  is the atmospheric pressure in hPa and  $P_0 = 1000$  hPa. The first term of equation (5) corresponds to the snow thermal conductivity [Anderson, 1976]. The second term represents the thermal conductivity from vapor transfer in the snow [Sun *et al.*, 1999]. Both soil  $C_p$  and soil  $k_j$  are prescribed as constants.  $\frac{\partial R}{\partial z}$ , which is not considered in ORCHIDEE, is the solar-radiative energy source term depending on snow depth, which is determined by

$$R(z) = R_0(1 - \alpha) \exp(-\gamma z) \quad (6)$$

Where  $R_0$  ( $\text{W m}^{-2}$ ) is incoming shortwave radiation,  $\alpha$  is the surface albedo, and  $\gamma$  ( $\text{m}^{-1}$ ) is the extinction coefficient for solar radiation.

### 2.2.3. Liquid Water Treatment

[9] For phase change processes, we use snow heat content ( $H_j$ ) defined as equation (7) [e.g., *Lynch-Stieglitz, 1994; Sun et al., 1999*] to allow the presence of either cold (dry) or warm (wet) snow. According to equation (7), heat content is used to diagnose the snow temperature assuming that there is no liquid water in the snow layer. If the calculated snow temperature in equation (4) exceeds the freezing point, snow temperature is set to freezing point, and liquid water content ( $LQW_j$ ) is then deduced from the following equation:

$$H_j = c_{sj}D_j(T_j - T_f) - L_f(W_j - LQW_j) \quad (7)$$

where  $W_j$  is the snow water equivalent at the  $j$ th layer.  $L_f$  is the latent heat fusion for ice ( $\text{J kg}^{-1}$ ).  $T_f$  is the triple point temperature for water.  $c_{sj}$  is snow heat capacity at  $j$ th layer, which is defined as a function of snow density ( $\rho_j$ ,  $\text{kg m}^{-3}$ ) and intrinsic density of ice ( $\rho_i = 920 \text{ kg m}^{-3}$ ) following *Verseghy [1991]*:

$$c_{sj} = 1.9 \times 10^6 \frac{\rho_j}{\rho_i} \quad (8)$$

[10] If the calculated snow temperature in equation (4) goes below freezing, liquid water in the  $j$ th layer partially or totally refreezes, and the energy released due to phase change is used to limit the cooling of this layer.

### 2.2.4. Mass Balance and Transfer

[11] Mass balance equations describe the change in total snow water equivalent in each layer, which is the sum of liquid water and ice content. The contribution of water vapor is neglected because of its unimportant role in the mass balance equation [*Sun et al., 1999*]. The mass balance of each snow layer can be expressed by the following equation.

$$\frac{\partial W_j}{\partial t} = \begin{cases} P_s + P_r - IF_j - R_j - E_n & (j = 1) \\ IF_{j-1} - IF_j - R_j & (j = 2, 3) \end{cases} \quad (9)$$

[12] In equation (9),  $W_j$  is the snow water equivalent (SWE) in the  $j$ th layer (m),  $P_s$  and  $P_r$  are snowfall and rainfall ( $\text{kg m}^{-2} \text{ s}^{-1}$ ) upon the first snow layer,  $R_j$  is runoff rate leaving the  $j$ th layer ( $\text{kg m}^{-2} \text{ s}^{-1}$ ), and  $E_n$  is the sum of evaporation and sublimation rate ( $\text{kg m}^{-2} \text{ s}^{-1}$ ).  $IF_j$  is the actual infiltration rate ( $\text{m s}^{-1}$ ) at the interface between the  $j$ th and ( $j + 1$ )th layer. Infiltration of liquid water into the next lower layer is controlled by maximum liquid water holding capacity. As such, melt water generated in a layer will remain in that layer if the liquid water content does not exceed the layer holding capacity. Otherwise, it will infiltrate down to the next lower layer where it may refreeze, remain in the layer in the liquid state, or pass through. The maximum liquid water holding capacity is taken as a function of the snow layer density following *Anderson [1976]*.

$$LQW_{j\max} = W_j \left[ rw_{\min} + (rw_{\max} - rw_{\min}) \max(0, \rho_t - \rho_j) / \rho_t \right] \quad (10)$$

where  $LQW_{j\max}$  is the maximum water holding capacity at the  $j$ th layer,  $rw_{\max} = 0.10$ ,  $rw_{\min} = 0.03$ , and  $\rho_t = 200 \text{ kg m}^{-3}$ .

### 2.2.5. Snow Compaction

[13] The compaction process is critically important for the evolution of the snow density and depth of each layer.

Snow depth is decreased by compaction, but it is increased by snowfall. The local rate of change of density (increase) due to the weight of the overlying snow and settling (primarily of new snowfall) is parameterized following *Anderson [1976]* as

$$\frac{1}{\rho_j} \frac{\partial \rho_j}{\partial t} = \frac{\sigma_j}{\eta_j(T_j, \rho_j)} + a_c \exp \left[ -b_c(T_f - T_j) - c_c \max(0, \rho_j - \rho_c) \right] \quad (11)$$

where the first term on the right-hand side of equation (11) represents overburden (the compactive viscosity term, see equation (12)). The pressure of the overlying snow is represented by  $\sigma$  (Pa), and  $\eta$  is the snow viscosity (Pa s), which is an exponential function of snow temperature and density (equation 12) [*Mellor, 1964; Kojima, 1967*]. The second term represents the metamorphism [*Anderson, 1976*] which can be significant for fresh relatively low-density snowfall. The values from *Anderson [1976]* are used:  $a_c = 2.8 \times 10^{-6} \text{ s}^{-1}$ ,  $b_c = 4.2 \times 10^{-2} \text{ K}^{-1}$ ,  $c_c = 460 \text{ m}^3 \text{ kg}^{-1}$ , and  $\rho_c = 150 \text{ kg m}^{-3}$ . The compaction constants can be treated as site-dependent calibration parameters, but they are held constant for all conditions and locations in the current model.

[14] The snow Newtonian viscosity is formulated as a function of snow density [*Kojima, 1967*] and temperature [*Mellor, 1964*] as

$$\eta_j = \eta_0 \exp \left[ a_\eta(T_f - T_j) + b_\eta \rho_j \right] \quad (12)$$

where  $\eta_0 = 3.7 \times 10^7 \text{ Pa s}$ ,  $a_\eta = 8.1 \times 10^{-2} \text{ K}^{-1}$ , and  $b_\eta = 1.8 \times 10^{-2} \text{ m}^3 \text{ kg}^{-1}$ .

### 2.2.6. Snow Albedo

[15] In ORCHIDEE-ES, for bare soil and short vegetation, snow albedo is parameterized using the following equation [*Boone and Etchevers, 2001*]:

$$\alpha_{gs}^{t+1} = (P_s \Delta t / W_{crn}) (\alpha_{\max} - \alpha_{\min}) + (1 - \omega_z) \left[ \alpha_{gs}^t - \tau_a \Delta t \right] + \omega_z \left[ (\alpha_{gs}^t - \alpha_{\min}) \exp(\tau_f \Delta t) + \alpha_{\min} \right] (\alpha_{\min} \leq \alpha_{gs} \leq \alpha_{\max}) \quad (13)$$

Where  $\alpha_{gs}^{t+1}$  and  $\alpha_{gs}^t$  denote the albedo of next and current time steps, and  $\alpha_{\min}$  and  $\alpha_{\max}$  minimum (0.50) and maximum snow albedo (0.85) values.  $\Delta t$  is the time step that is expressed in days, and  $P_s$  is snow fall amount (mm). A linear decrease rate is used for dry snow ( $\tau_a = 0.008 \text{ s}$ ) [*Baker et al., 1990*], and an exponential decrease rate ( $\tau_f = 0.24 \text{ s}$ ) is used to model the wet metamorphism [*Verseghy, 1991*]. The weight  $\omega_z$  is defined as the degree of saturation, which is the ratio of snow liquid content to snow water equivalent in the surface snow layer. The snow albedo increases at a rate proportional to snowfall. A snowfall of at least 10 cm water equivalent ( $W_{crn} = 10 \text{ cm}$ ) resets the snow albedo back to its maximum value. The total surface albedo on short vegetations or bare soil ( $\alpha_{\text{surf}}$ ) is then computed as the sum of the snow-free vegetation or bare-soil albedo ( $\alpha_{gs}$ ) [*Chalita*

and *Le Treut*, 1994] and snow-covered albedo ( $\alpha_{gs}$ ), which is weighted by the snow cover fraction ( $f_{sg}$ ).

$$\alpha_{\text{surf}} = f_{sg}\alpha_{gs} + (1 - f_{sg})\alpha_{gns} \quad (14)$$

[16] The snow cover fraction on each grid box ( $f_{sg}$ ) is a function of total SWE (the sum of  $W_j$  from each layer), as given by the following:

$$f_{sg} = \text{SWE}/(\text{SWE} + 10) \quad (15)$$

In this study, for site simulations focusing on snow physics, we force  $f_{sg}$  to 1 as soon as the snowpack reaches the low user-defined SWE threshold ( $10 \text{ kg m}^{-2}$ ).

[17] To test the impacts of the albedo parameterization on snow simulations, the default snow albedo scheme in ORCHIDEE has been replaced by equation (13) (called ORCHIDEE-ALB hereafter). In equation (13), the fraction of liquid water in the surface layer is used to denote the snow state (wet versus dry), because the wet snow is parameterized to have a larger snow albedo decay rate than the dry snow. Given that liquid water is not accounted for in ORCHIDEE-ALB, instead of using the fraction of liquid water in the surface layer, skin layer temperature in ORCHIDEE-ALB is used as a proxy for snow state (wet versus dry), e.g., snow is diagnosed as wet when skin layer temperature is above  $0^\circ\text{C}$ .

### 2.2.7. Snow Effects on Roughness Length

[18] In ORCHIDEE-ES, the impact of snow cover on surface roughness has been added. Snow cover is assumed to reduce the gridbox effective roughness length following the averaging method from *Noilhan and Lacarrère* [1995].

$$\frac{1}{\ln[z_r/z_{0t}]^2} = \frac{f_{sg}}{\ln[z_r/z_{0n}]^2} + \frac{1-f_{sg}}{\ln[z_r/z_0]^2} \quad (16)$$

where  $f_{sg}$  is snow cover fraction,  $z_{0t}$  is surface roughness length after considering snow cover,  $z_0$  is the vegetation or surface roughness length (m),  $z_{0n}$  is the snow surface roughness length baseline value ( $0.001 \text{ m}$ ), and  $z_r$  is the blending height ( $10 \text{ m}$  in ORCHIDEE-ES).

## 3. Model Performance

[19] The model performances are evaluated with several metrics. The temporal correlations between observed and modeled snow variables make use of correlation coefficient  $r$ .

$$r = \frac{\sum (P_i - \bar{P})(O_i - \bar{O})}{\sqrt{\sum (P_i - \bar{P})^2} \sqrt{\sum (O_i - \bar{O})^2}} \quad (17)$$

where  $O_i$  is observed variable,  $P_i$  is modeled variable, and  $\bar{O}$  and  $\bar{P}$  denote means of observed and modeled variables, respectively. The correlation coefficient is a direct measure of how well the observations and simulations vary jointly in time. The mean bias error (MBE) and the root mean square error (RMSE) have also been calculated. On the one hand, MBE calculation provides an estimate of whether the model has the tendency to overpredict (e.g., positive bias) or underpredict (e.g., negative bias) snow variables with respect to observations. On the other hand, the RMSE

is a measure of the deviation between the model and the observations. MBE is given by the following:

$$\text{MBE} = \frac{1}{N} \sum_{i=1}^n (P_i - O_i) \quad (18)$$

where  $N$  is the number of observations,  $O_i$  is observed variable, and  $P_i$  is modeled variable. RMSE, which is used to quantify the accuracy of the simulations, has been computed as follows:

$$\text{RMSE} = \sqrt{\frac{1}{N} \sum_{i=1}^n (P_i - O_i)^2} \quad (19)$$

where  $O_i$  is observed data,  $P_i$  is modeled data, and  $\bar{O}$  is mean of observed data.

[20] In addition, RMSE reduction ratio (RMSE-RR) is calculated as the following equation,

$$\text{RMSE-RR} = \frac{\text{RMSE}_{\text{ORCHIDEE}} - \text{RMSE}_{\text{ORCHIDEE-ES}}}{\text{RMSE}_{\text{ORCHIDEE}} + \text{RMSE}_{\text{ORCHIDEE-ES}}} \times 2.0 \quad (20)$$

where  $\text{RMSE}_{\text{ORCHIDEE}}$  ( $\text{RMSE}_{\text{ORCHIDEE-ES}}$ ) are the RMSEs between modeled and observed target variables, calculated for the two models, respectively. Positive RMSE-RR indicates that ORCHIDEE-ES improves target variable simulation, and negative RMSE-RR represents that ORCHIDEE-ES degrades the simulation.

## 4. Model Evaluation at the Col de Porte Site (1993–2011)

### 4.1. Site Description

[21] The Col de Porte (CDP) experimental site ( $1325 \text{ m}$  altitude,  $45^\circ 17' \text{N}$ ,  $05^\circ 45' \text{E}$ ) is situated in the Chartreuse mountain range near Grenoble, France. It is located in a grassy meadow surrounded by a coniferous forest and has been used for over 50 years as an experimental field site devoted to the study of snow in mountains. The snow often begins in November and ends at the beginning of May. The air temperature can intermittently exceed the freezing point throughout the winter, and rainfall episodes are common during the snow season. The soil generally does not freeze. This site has been widely used to evaluate snow schemes [e.g., *Brun et al.*, 1992; *Sun et al.*, 1999; *Essery et al.*, 1999, 2013; *Boone and Etchevers*, 2001; *Essery and Etchevers*, 2004; *Etchevers et al.*, 2004; *Brown et al.*, 2006; *Vionnet et al.*, 2012].

[22] The CDP meteorological data are quality controlled only for the periods when snowfall happens. Outside this time interval, the meteorological data are replaced by the output of the SAFRAN analysis system [*Durand et al.*, 1993]. A forcing data set at hourly timescale covering the period from 1 August 1993 to 31 July 2011 has then been built for the purpose of simulations spanning the entire year [*Morin et al.*, 2012]. For model simulations, we perform an 18 year spin-up starting on 1 August 1993 and then use the state variables from 31 July 2011 as the initial state for a new set of simulations starting on 1 August 1993.

[23] The in situ hourly snow surface temperature from a downward-looking radiometer, hourly snow depth from an ultrasonic sensor, and daily bottom runoff from snowpack measured by a  $5 \text{ m}^2$  lysimeter are used for model evaluation. We also use daily SWE measured using a ground-based

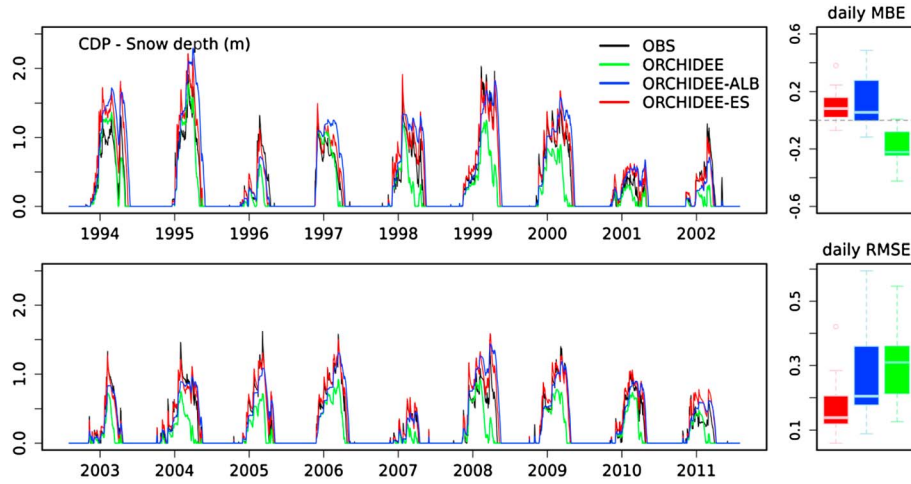


**Figure 2.** Daily snow depth comparisons between observation and simulations at CDP during the period 1993–2011. The daily MBE and RMSE during the period from December to May across years are shown in box plot. The bottom and the top of the box denote the 25th and 75th percentiles, respectively, and the band near the middle of the box is the 50th percentile (the median).

cosmic rays counter [Kodama *et al.*, 1979; Paquet and Laval, 2006]. Note that this instrument is calibrated using manual measurements of SWE, which are carried out on a weekly basis. The resulting uncertainty is of the order of 10% [Morin *et al.*, 2012]. In addition, the total snow density obtained by dividing the observed SWE with snow depth on weekly timescale is also used. Full details regarding the data set are given in Morin *et al.* [2012].

**4.2. Evaluation of Snow Variables and Temperatures**

[24] This section provides the evaluation results using five snow variables (snow depth, SWE, snow density, snow albedo, and snowmelt runoff) and the two temperatures (surface temperature and 10 cm soil temperature). All data are averaged over pentads in order to display seasonal evolution of snow albedo, snowmelt runoff, and the two temperatures. For error statistics (MBE and RMSE), both snow albedo and snowmelt runoff are calculated on a daily basis, and the two temperatures are computed on an hourly basis.

**4.2.1. Snow Depth and SWE**

[25] As shown in Figures 2 and 3, ORCHIDEE-ES improves daily snow depth and daily SWE simulations at CDP. The daily MBE from December to May has been reduced from ORCHIDEE (snow depth:  $-0.19 \pm 0.12$  m; SWE:  $-91 \pm 39$  kg m<sup>-2</sup>) to ORCHIDEE-ES (snow depth:  $0.09 \pm 0.12$  m; SWE:  $-17 \pm 37$  kg m<sup>-2</sup>). The daily RMSE from December to May has also been reduced from ORCHIDEE (snow depth:  $0.30 \pm 0.11$  m; SWE:  $132 \pm 39$  kg m<sup>-2</sup>) to ORCHIDEE-ES (snow depth:  $0.17 \pm 0.10$  m; SWE:  $41 \pm 22$  kg m<sup>-2</sup>). The values behind the sign  $\pm$  are standard deviation across years. Our results are comparable to those of the Vionnet *et al.* [2012] study, which reports that the MBE (RMSE) values in ISBA-ES are 0.06 (0.12 m) and  $-12$  ( $41$  kg m<sup>-2</sup>) for snow depth and SWE over the period 2000–2011, respectively.

**4.2.2. Snow Density**

[26] Figure 4 shows that observed snow density on a weekly basis is well captured by ORCHIDEE-ES ( $r=0.83$ , MBE =  $-18$  kg m<sup>-3</sup>, RMSE =  $48$  kg m<sup>-3</sup>) from all samples

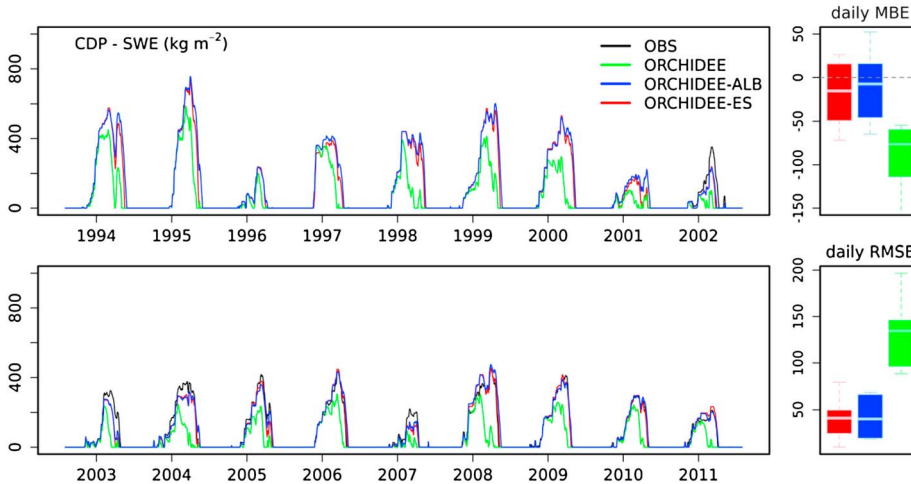


**Figure 3.** Daily SWE comparisons between observation and simulations at CDP during the period 1993–2011. The meaning of box plot is the same with Figure 2.

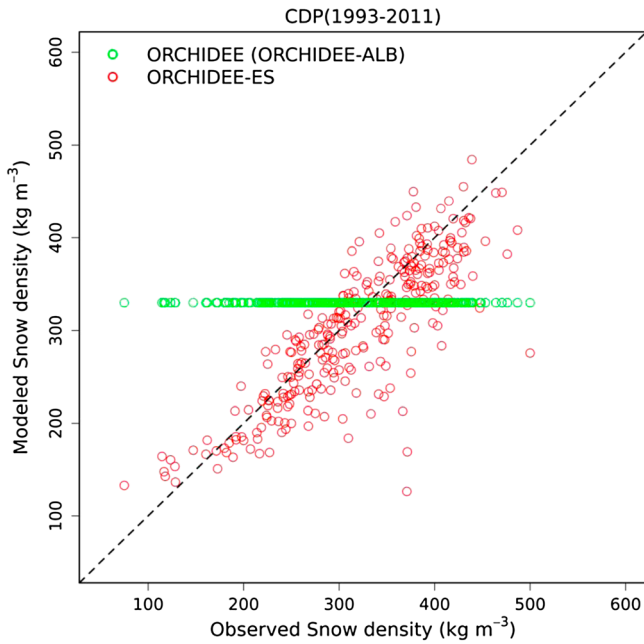


**Figure 4.** Scatter plot of weekly snow density between observation and simulations across all points from 1993 to 2011.

during the period 1993–2011. By contrast, snow density is prescribed constant in ORCHIDEE ( $330 \text{ kg m}^{-3}$ ). A more realistic snow density simulation in ORCHIDEE-ES is critical because it impacts snow thermal conductivity [e.g., *Sturm et al., 1997, Calonne et al., 2011*]. However, snow density and snow thermal conductivity in ORCHIDEE are independently prescribed as constants. Utilizing ORCHIDEE with an added permafrost module [*Koven et al., 2009*], *Gouttevin et al. [2012a]* prescribed observed snow density (and snow thermal conductivity) for two contrasted snow classes (tundra and taiga in their case) over the pan-arctic region and found soil carbon stocks to be 8% lower than with uniform snow density and thermal conductivity. This highlights the necessity to model the spatial distribution of snow density and thermal conductivity. The *Gouttevin et al. [2012a]* study was rather idealized, because only two snow classes were distinguished

for the pan-arctic region. Further details can be brought by ORCHIDEE-ES, in which snow density is calculated and snow thermal conductivity is parameterized as a function of snow density [e.g., *Yen, 1981; Sturm et al., 1997; Calonne et al., 2011*]. However, snow density may also be governed by other drivers (e.g., wind speed, vegetation types), which are not currently considered.

**4.2.3. Snow Albedo**

[27] As shown in Figure 5, the seasonal evolution of snow albedo from December to May in pentads is captured by both ORCHIDEE and ORCHIDEE-ES. One can observe that ORCHIDEE-ES (MBE =  $0.04 \pm 0.06$ ; RMSE =  $0.11 \pm 0.03$ ) better simulates daily snow albedo compared to ORCHIDEE (MBE =  $-0.18 \pm 0.04$ ; RMSE =  $0.22 \pm 0.03$ ). During the early winter and spring seasons, a residual bias is seen in simulated snow albedo from ORCHIDEE-ES (Figure 5). This is related to a shortcoming of the model in reproducing the start and end of snow season. In addition, accurate representation of snow albedo is very important since our following results (section 4.3.1) indicate that the bias in the simulated snow depth and SWE by ORCHIDEE is partly explained from the snow albedo underestimation.

**4.2.4. Snowmelt Runoff**

[28] Figure 6 compares observed and modeled snowmelt runoff between ORCHIDEE and ORCHIDEE-ES. The timing and total amount of snowmelt runoff is better simulated by ORCHIDEE-ES which has a lower RMSE ( $9.3 \pm 1.7 \text{ mm}$ ) and a smaller MBE (underestimation) ( $-0.7 \pm 1.7 \text{ mm}$ ) than ORCHIDEE (RMSE:  $11.2 \pm 2.2 \text{ mm}$ ; MBE:  $-0.9 \pm 1.8 \text{ mm}$ ). Although ORCHIDEE shows a similar runoff behavior than the observations, ORCHIDEE-ES is found to track more closely the changes in snowmelt runoff during the mid-ablation season and final melting season. Moreover, the timing of snowmelt runoff peak in ORCHIDEE occurs much earlier than that from ORCHIDEE-ES and the observations.

**4.2.5. Snow Surface Temperature**

[29] Both models are capable of simulating the seasonal dynamics of snow surface temperature (Figure 7). Besides the snow season (December–May), hourly error statistics (RMSE and MBE) are calculated for the two models during the “common snow period” where models and data have at least 5 cm snow depth. Figure 7 shows that the difference

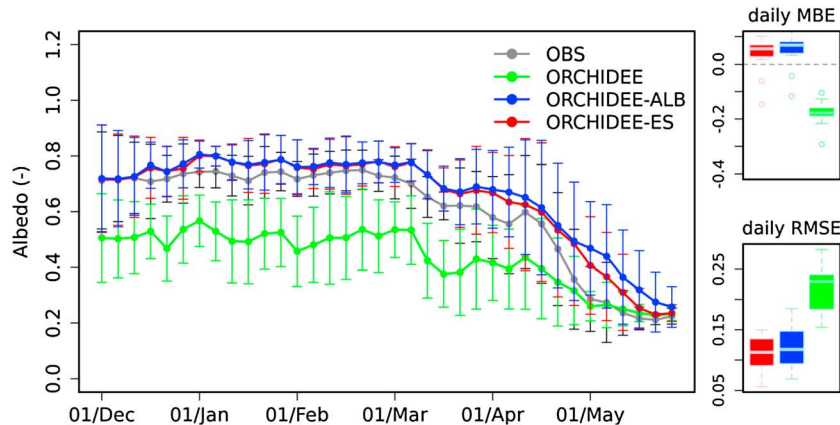


**Figure 5.** Comparison of multiyear averaged (1993–2011) snow albedo in pentads between observation and simulations during the period from December to May at CDP. For each pentad, the error bar denotes standard deviation of albedo values from all available years. The meaning of box plot is the same with Figure 2.

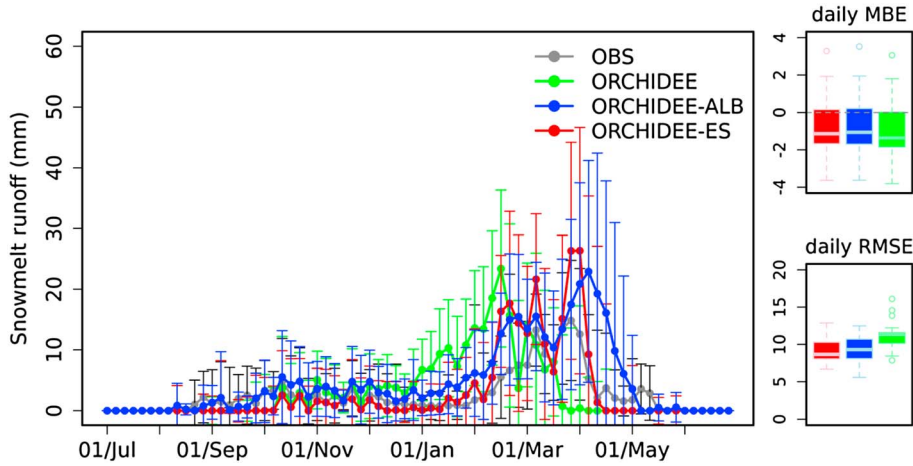


**Figure 6.** Comparison of multiyear averaged (1993–2011) snowmelt runoff in pentads between observation and simulations at CDP. For each pentad, the error bar denotes standard deviation of snowmelt runoff from all available years. The meaning of box plot is the same with Figure 2.

between hourly error statistics of the two models is smaller during common snow period than during the whole period (December–May). This can be expected because ORCHIDEE predicts an earlier snow disappearance, and then, the temperature resulting from the surface energy budget is not the true snow surface temperature. When a common snow period is considered, ORCHIDEE-ES has a cold bias ( $-0.8 \pm 0.6^\circ\text{C}$ ), but ORCHIDEE has a warm bias ( $0.4 \pm 0.5^\circ\text{C}$ ). The warm bias in ORCHIDEE is related to the underestimated snow albedo (section 4.3.1). The cold bias of ORCHIDEE-ES is also found in other intermediate complexity snow models [e.g., Essery and Etchevers, 2004; Brown *et al.*, 2006] and may reflect the fact that the Monin-Obukhov similarity theory implemented in these land surface models is unable to explain turbulent energy exchanges over snow and ice under stable

atmospheric conditions [Martin and Lejeune, 1998]. Even under stable atmospheric conditions, turbulence still exists and is characterized by intermittent bursts. As explored in detail by Brown *et al.* [2006], an inclusion of windless transfer coefficient in the sensible heat flux calculation may partly rectify the cold bias in surface temperature.

**4.2.6. Soil Temperature**

[30] The simulation for soil temperature at the depth of 10 cm is improved in ORCHIDEE-ES in comparison to ORCHIDEE, as shown in Figure 8. For example, during the common snow period, hourly MBE and hourly RMSE are reduced from  $-4.3 \pm 1.1^\circ\text{C}$  and  $5.5 \pm 1.2^\circ\text{C}$  in ORCHIDEE to  $-1.0 \pm 0.9^\circ\text{C}$  and  $1.7 \pm 0.9^\circ\text{C}$  in ORCHIDEE-ES, respectively. A parameterization of snow thermal conductivity based on snow density in ORCHIDEE-ES contributes to enhanced

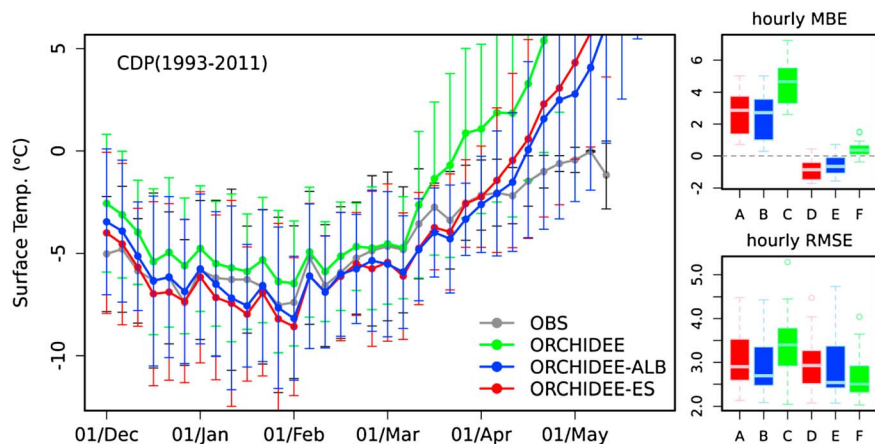


**Figure 7.** Comparison of multiyear averaged (1993–2011) snow surface temperature in pentads between observation and simulations during the period from December to May at CDP. For each pentad, the error bar denotes standard deviation of snow surface temperature from all available years. The meaning of box plot is the same with Figure 2, but MBE and RMSE are computed on the hourly basis. A, B, and C denote error statistics calculation that is performed on the whole period (December–May) for ORCHIDEE-ES, ORCHIDEE-ALB, and ORCHIDEE, respectively; D, E, and F denote error statistics calculation that is performed on the common snow period (see text for explanation) for ORCHIDEE-ES, ORCHIDEE-ALB, and ORCHIDEE, respectively.

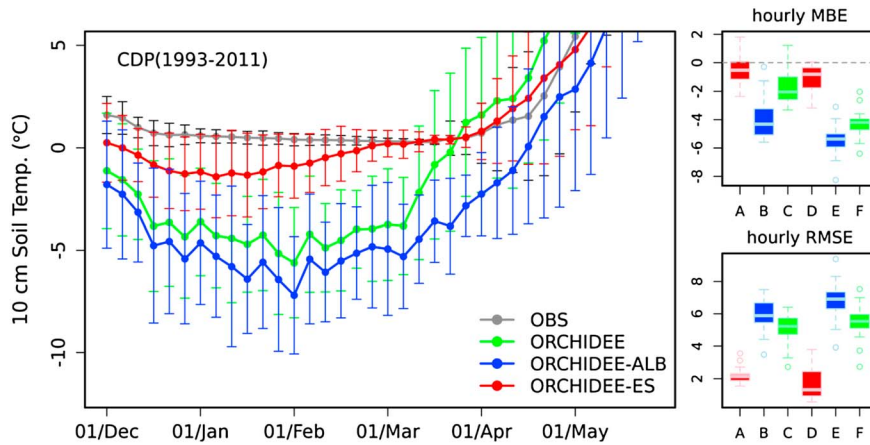


**Figure 8.** Comparison of multiyear averaged (1993–2011) soil temperature at the depth of 10 cm in pentads between observation and simulations during the period from December to May at CDP. The explanation on error bar, boxplot and letters (A, B, C, D, E and F) is referenced to Figure 7.

behaviors in soil temperature simulation. This might be implied from the results of a sensitivity analysis based on Morris method for parameter ranking, which shows that parameters related to snow thermal conductivity are the second highest sensitive (important) in ORCHIDEE-ES soil temperature simulations (see details in section 4.3.2). In addition, ORCHIDEE has only one single snow layer, not allowing the temperature gradients within the snowpack, which produces a bias in the ground heat flux and soil temperature, because temperature at the bottom of the snow pack is less variable than that near the snow surface (large diurnal cycle). ORCHIDEE-ES better accounts for the vertical propagation of the surface heat wave into the snowpack through the soil, since it represents vertical gradients of snow thermal conductivity with snow density. Finally, ORCHIDEE has a mixed soil-snow structure, where the snow temperature is assumed to be equal to the temperature of the first soil layer. The separation of bottom snow layer from first soil layer in ORCHIDEE-ES allows distinguished thermal conductivity between them, which can also contribute to improve soil temperature simulation. However, we should emphasize that snow albedo parameterizations in ORCHIDEE-ES do not really benefit soil temperature simulation (see details in section 4.3.1). The cold bias in simulated soil temperature still persists in ORCHIDEE-ES, which is possibly related to other missing processes (e.g., inaccurate settings of CDP soil thermal parameters, soil freezing/thawing processes, soil thermal insulation by soil carbon).

**4.3. Sensitivity Tests**

**4.3.1. Sensitivity to Snow Albedo**

[31] In order to investigate how snow albedo alone changes the other snow variables, we replaced the snow albedo scheme in ORCHIDEE with a modified one from ORCHIDEE-ES (named as ORCHIDEE-ALB, section 2.2.6). In ORCHIDEE-ALB, snow albedo simulation has been largely improved, for example, daily RMSE has been reduced from  $0.22 \pm 0.03$  to  $0.12 \pm 0.03$ . Moreover, RMSEs concerned with simulated snow depth, SWE, and snowmelt runoff are smaller with ORCHIDEE-ALB than those from ORCHIDEE (Table 1). However, the improvement of snow depth brought by a better albedo scheme alone is not as large as that observed in SWE and snowmelt runoff. This could be expected since constant snow density is still adopted in ORCHIDEE-ALB. This result confirms that the representation of snowpack internal processes is necessary [Essery et al., 2013]. Moreover, soil temperature underlying the snow pack in ORCHIDEE-ALB still stays colder than the observations. Instead, soil temperature simulation in ORCHIDEE-ALB is degraded (Table 1 and Figure 8). This is because ORCHIDEE-ALB simulates a higher snow albedo and a colder surface temperature (then soil temperature) than ORCHIDEE (Table 1). Both hourly MBE and hourly RMSE are very high in ORCHIDEE-ALB (Table 1). In addition, in contrast to ORCHIDEE ( $0.4 \pm 0.5^\circ\text{C}$ ), MBE in snow surface temperature is negative in ORCHIDEE-ALB ( $-0.5 \pm 0.6^\circ\text{C}$ ),

**Table 1.** Summary of MBE and RMSE for Different Snow Variables and the Two Temperatures at Col de Porte<sup>a</sup>

	MBE			RMSE		
	ORCHIDEE	ORCHIDEE-ALB	ORCHIDEE-ES	ORCHIDEE	ORCHIDEE-ALB	ORCHIDEE-ES
Snow Depth (m)	-0.19 (0.12)	0.12 (0.17)	0.09 (0.12)	0.29 (0.11)	0.26 (0.14)	0.17 (0.10)
SWE ( $\text{kg m}^{-2}$ )	-91 (39)	-11 (38)	-17 (37)	132 (39)	41 (22)	42 (20)
Snow Albedo	-0.18 (0.04)	0.05 (0.05)	0.04 (0.06)	0.22 (0.03)	0.12 (0.03)	0.11 (0.03)
Surface Temp. ( $^\circ\text{C}$ )	0.4 (0.5)	-0.5 (0.6)	-0.8 (0.6)	2.7 (0.6)	3.0 (0.9)	3.0 (0.7)
10 cm Soil Temp. ( $^\circ\text{C}$ )	-4.3 (1.1)	-5.5 (1.2)	-1.0 (0.9)	5.5 (1.2)	6.7 (1.3)	1.7 (0.9)
Snowmelt Runoff (mm)	-0.9 (1.8)	-0.7 (1.8)	-0.7 (1.8)	11.2 (2.2)	9.1 (1.9)	9.3 (1.7)

<sup>a</sup>The values in parenthesis denote the standard deviation across years. The error statistics for snow depth, SWE, and snow albedo are calculated during the period from October to May. The error statistics for surface temperature and 10 cm soil temperature are calculated during the common snow period. The error statistics for snowmelt runoff are calculated during the full year.

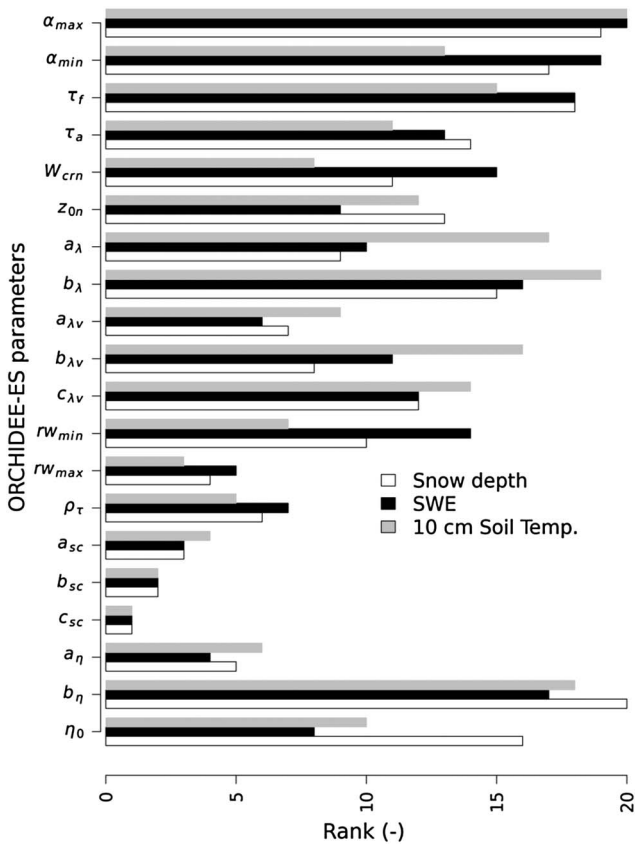


**Figure 9.** Ranking of the parameters in ORCHIDEE-ES based on the Morris method at CDP when studying snow depth (m), SWE ( $\text{kg m}^{-2}$ ), and 10 cm soil temperature ( $^{\circ}\text{C}$ ). The importance of the parameter is represented by the bar length (the larger the bar, the more importance the parameter).

which is also found in ORCHIDEE-ES ( $-0.8 \pm 0.6^{\circ}\text{C}$ ). This implies that the warm bias of snow surface temperature found in ORCHIDEE is predominantly related to snow albedo underestimation (Figure 5).

[32] This sensitivity analysis emphasizes the predominant sensitivity of snow albedo in the simulation of other snow variables, which implies that both snowpack and hydrological variables could benefit from realistic snow albedo, e.g., that could be assimilated from satellite measurements [e.g., Malik et al., 2012]. This is particularly relevant since other contributing factors (e.g., black carbon, wind-driven surface microtopography) on snow albedo may be implicitly included in satellite-derived albedo observations.

**4.3.2. Parameter Sensitivity Tests in ORCHIDEE-ES**

[33] Understanding the relative importance of parameters when implementing new parameterizations can give insights into the uncertainty in simulations and provide guidelines for further model refinements. In order to better understand the relative importance of the new processes represented, the Morris method [Morris, 1991] is adopted to rank the parameters of the ORCHIDEE-ES snow model. This method is based on a screening approach which consists in analyzing the behavior of output variables when varying the parameter values in a predefined parameter space. Its implementation is fully described in Appendix A. The 20 parameters are grouped in five categories (snow albedo, roughness length,

snow thermal properties, snow water holding capacity, and snow compaction) which were found to have influences on snow simulations in previous studies [e.g., Essery et al., 1999, 2013; Boone and Etchevers, 2001; Essery and Etchevers, 2004; Etchevers et al., 2004; Brown et al., 2006].

[34] Figure 9 displays the parameter ranking in ORCHIDEE-ES at CDP when studying snow depth, SWE, and 10 cm soil temperature variables (the larger the bar, the more important the parameter). The results confirm that the parameters related to snow albedo parameterization (minimum and maximum snow albedo values and albedo decay rate for melting snow) play important roles on the simulation of these output variables. This was also found in previous studies [Essery and Etchevers, 2004]. The parameter  $\tau_f$  used to describe snow albedo decay rate during melting season, which plays an important role when studying snow water equivalent in the model, can be understood as a proxy variable for snow grain size and impurity content and their evolution. Indeed, the most physical way to approach the construction of a snow albedo parameterization is to incorporate snow grain size prognostically and relate snow albedo to grain size evolution [e.g., Brun et al., 1989; Kuipers Munneke et al., 2011]. However, our snow albedo parameterization is still empirical, and the parameter  $\tau_f$  as a proxy of grain size evolution is very sensitive. Our study thus highlights the necessity of considering snow grain size in further developments.

[35] Our results also reveal the dominance of the parameters ( $\eta_0$  and  $b_\eta$ ) controlling compaction rate over the others, especially with respect to snow depth. In fact, the compaction rate for a given overburden pressure mainly depends on the thermal state of snow pack, which varies locally but mainly as a function of local meteorological conditions. The large sensitivities found in parameters related to compaction rate lead us to suggest that the uncertainty of snow depth simulations can be greatly constrained if snow compaction rates can be physically approached in the model.

[36] The parameters ( $a_\lambda$  and  $b_\lambda$ ) controlling snow ice thermal conductivity are also identified as important regulators able to outcompete some parameters especially in soil temperature simulation (Figure 9). In contrast, the parameters ( $a_{\lambda v}$  and  $b_{\lambda v}$ ) related to heat transfer through snow by interstitial air conduction are less sensitive in the model. Previous studies justify the application of simple regression curves between snow ice thermal conductivity and snow density in snow models [e.g., Yen, 1981; Sturm et al., 1997; Calonne et al., 2011]. However, such regression curves differ widely, and there is up to a factor of 2 between different studies [Yen, 1981; Sturm et al., 1997]. Our sensitivity analysis highlights that the regression parameters ( $a_\lambda$  and  $b_\lambda$ ) linking these two variables should be further constrained in future experimental studies by considering a wide range of snow types and a common experimental design [e.g., Calonne et al., 2011].

[37] However, we should keep in mind that the parameter ranking obtained for snow simulation in CDP site might not be directly transferred to other sites. This needs further verification in future studies mainly designed for parameter sensitivity analysis. Moreover, the Morris method is indeed a screening method to identify influential and non-influential parameters in the model without any quantitative information. This means that the quantitative measure of the influence of specific parameter cannot be identified. The current analysis

can still provide valuable information on the importance of parameters in ORCHIDEE-ES snow simulations, which can prepare future model calibration only using the identified most sensitive parameters.

## 5. Model Evaluation in Northern Eurasia

### 5.1. Data Description

[38] In order to evaluate the snow model performances on the large spatial scale, we use ground snow observations from both Historical Soviet Daily Snow Depth (HSDSD) [Armstrong, 2001] and Former Soviet Union Hydrological Snow Surveys (FSUHSS) [Krenke, 2004] data sets. HSDSD includes quality controlled daily snow depth data that have been collected in open areas or clearings in forest regions. We consider 263 stations located in a northern Eurasian domain extending from 30.5°W to 180°W and from 35.5 to 73.5°N, with daily snow depth observations, half of them without any missing data. FSUHSS includes additional snow density, snow depth, and SWE observations [Brun *et al.*, 2013]. The data source for evaluating model performance in near-surface soil temperature simulations comes from monthly soil temperature at 20 cm depth, which is available in the Russia Historical Soil Temperature Data TMD2 data set [Zhang *et al.*, 2001]. For this comparison, we use only stations that are collocated with the HSDSD or FSUHSS snow observations.

### 5.2. Model Forcing and Simulations

[39] The meteorological variables for driving ORCHIDEE are extracted from the ERA-Interim [Dee *et al.*, 2011] reanalysis at the grid point of each station. ERA-Interim reanalysis has a good quality of snowfall chronology since cold season precipitation over northern Eurasia is mainly caused by synoptic-scale systems with mostly stratiform type precipitation, which are well captured by this product [Brun *et al.*, 2013]. Global Precipitation Climate Center (GPCC) gridded monthly precipitation (Full Data Product V5) is employed as a scaling factor for monthly ERA-Interim precipitation. This data set is chosen given that the best snow model performance when blowing snow is not represented has been obtained using GPCC-scaling ERA-Interim precipitation [Brun *et al.*, 2013]. We choose the period extending from 1 July 1979 to 30 June 1993, which combines the availability of ERA-Interim data sets together with a large number of stations' snow depth records. The elevation difference between each station and the corresponding grid box from ERA-Interim has been considered in generating meteorological variables used for driving ORCHIDEE (see Brun *et al.* [2013] for details). In addition, we adopt a snow-rain partitioning threshold equal to 1°C. At each station, the vegetation type is prescribed as grassland in the model. We first perform a 14 year spin-up starting on 1 July 1979 and then use the soil temperature profile on 30 June 1993 as the initial state for a new set of simulations starting on 1 July 1979.

### 5.3. Statistical Analysis

[40] To evaluate model performance in snow depth simulation, more than 1,100,000 daily snow depth observations from all station years have been employed to calculate the error statistics (MBE, RMSE, and  $r$ ). For SWE, more than 100,000 observations have been used. In addition, we only

consider the stations which have at least 10 years of near complete (at least 360 days) year-round snow depth observations (165 stations satisfy this criterion). They are used to evaluate the model performance in capturing spatio-temporal variability of snow depth in northern Eurasia. Moreover, these observations are also used to define start and end dates of the longest period with continuous snow on the ground (defined as snow depth higher than 0.5 cm), which are then compared to modeled values.

[41] The monthly observed soil temperature from the TMD2 data set is recorded at the depth of 20 cm, which does not correspond to the modeled soil discretization. Thus, we linearly interpolate soil temperature between 12.9 and 30.1 cm model depths. This simple linear interpolation might result in a cold bias [e.g., Gouttevin *et al.*, 2012b, Figure 3]. Comparison between monthly observed and modeled soil temperature is conducted during three winter months (December throughout February). In order to investigate whether the performance of ORCHIDEE-ES compared to ORCHIDEE for soil temperature simulation depends on snow depth, the RMSE reduction ratio (RMSE-RR, equation (20)) is regressed against mean snow depth across stations each winter month. In equation (20),  $RMSE_{ORCHIDEE}$  ( $RMSE_{ORCHIDEE-ES}$ ) is the RMSE between modeled and observed monthly soil temperature at 20 cm depth across at least 10 years for each winter month.

### 5.4. Evaluation of Snow Variables

[42] Over all stations, snow depth, SWE, and snow density are simulated more accurately in ORCHIDEE-ES (lower RMSE and higher  $r$ ) than ORCHIDEE (Table 2). The RMSE between modeled and observed daily snow depth (m) decreases from 0.12 in ORCHIDEE to 0.10 in ORCHIDEE-ES, and the RMSE for daily SWE ( $kg\ m^{-2}$ ) decreases from 49.8 in ORCHIDEE to 44.2 in ORCHIDEE-ES. The largest RMSE reduction (RMSE-RR) and the highest  $r$  increment from ORCHIDEE to ORCHIDEE-ES are obtained for snow density that is prescribed constant ( $330\ kg\ m^{-3}$ ) in ORCHIDEE. In addition, snow depth has a higher RMSE-RR (18%) than SWE (12%), which is in support of our previous analysis at CDP site.

[43] Across the 165 northern Eurasian stations with near complete year-round snow depth observations (Figure 10a), both models could capture interannual variability in annual snow depth well, in terms of  $r$  (ORCHIDEE-ES:  $r$  ranges from 0.57 to 0.89 versus ORCHIDEE:  $r$  ranges from 0.56 to 0.88) (Figure 10b). The range values in parenthesis denote the 25th and 75th percentiles. In terms of RMSE and MBE, ORCHIDEE ( $0.11 \pm 0.08\ m$  and  $-0.10 \pm 0.08\ m$ ) displays worse performances than ORCHIDEE-ES ( $0.07 \pm 0.07\ m$  and  $-0.003 \pm 0.08\ m$ ) in snow depth. The values behind the sign  $\pm$  are standard deviation across stations. This is also found if we compare the two models in the simulation of spatial variation of multiyear averaged annual snow depth across 165 stations (Figure 10c). These spatio-temporal model evaluations indicate that ORCHIDEE has a systematic underestimation of snow depth because of unrealistic snow albedo representation and absent prognostic snow density (section 4.2.1). Furthermore, ORCHIDEE-ES has a more realistic representation of start and end dates of continuous snow cover than ORCHIDEE when confronting the model output against the observation across all station years (Table 2). For example, the mean bias for end date of snow cover is of 3 days

**Table 2.** The Summary of Statistics (MBE, RMSE, and  $r$ ) for Snow Variables Simulated by Two Snow Models (ORCHIDEE and ORCHIDEE-ES) Over Northern Eurasia Stations<sup>a</sup>

Variable	N	Statistics	ORCHIDEE	ORCHIDEE-ES
Snow depth (m)	1,016,981	MBE	-0.05	-0.00
		RMSE	0.12	0.10
		$r$	0.78	0.83
Snow water equivalent ( $\text{kg m}^{-2}$ )	113,113	MBE	-22.7	-4.9
		RMSE	49.8	44.2
		$r$	0.60	0.66
Snow density ( $\text{kg m}^{-3}$ )	41,852	MBE	76.0	-24.3
		RMSE	92.8	53.6
		$r$	0.00	0.55
Start of continuous snow cover (days)	2,141	MBE	7	1
		RMSE	18	15
		$r$	0.87	0.89
End of continuous snow cover (days)	2,141	MBE	-10	3
		RMSE	20	18
		$r$	0.85	0.86

<sup>a</sup>For the onset date, the end date, and density, the statistical computation over each station and each year requires that both observations and simulations show a snow depth larger than a prescribed threshold (0.005 m for onset and end dates at least once in the year, 0.1 m for density).

in ORCHIDEE-ES, which is smaller than the -10 days obtained in ORCHIDEE. This indicates that ORCHIDEE-ES better represents the presence/absence of snow on the surface, which is critical for snow-climate feedbacks.

[44] ORCHIDEE-ES has a negative bias in SWE ( $-4.9 \text{ kg m}^{-2}$ ) and a near zero bias in snow depth (0.001 m) simulations (Table 2). This is comparable to the result (SWE:  $2.3 \text{ kg m}^{-2}$ ; snow depth: 0.008 m) from Brun *et al.* [2013], using the same data sets but a more complex physical snow model Crocus. Note that the sources of simulation bias in ORCHIDEE-ES might stem from the fixed snowfall threshold air temperature ( $1^\circ\text{C}$ ) and/or the inaccuracy of ERA-Interim precipitation in mountainous regions as already noted by Brun *et al.* [2013].

### 5.5. Evaluation of Near-Surface Soil Temperature

[45] Figure 11b shows the scatter plot between observed and modeled monthly soil temperature at the depth of 20 cm. Each point denotes a monthly averaged value. ORCHIDEE-ES generally improves monthly 20 cm soil temperature simulations during the winter season (December throughout February) in terms of the statistics used for measuring the model performance. For example, the RMSE decreases from  $10.5^\circ\text{C}$  to  $7.9^\circ\text{C}$ , and MBE changes from  $-9.4^\circ\text{C}$  to  $-6.3^\circ\text{C}$ . This could be attributed to the fact that thermo-insulation effect of snow on soil could be more realistically approached by ORCHIDEE-ES than ORCHIDEE. The better simulation of soil temperature in ORCHIDEE-ES provides

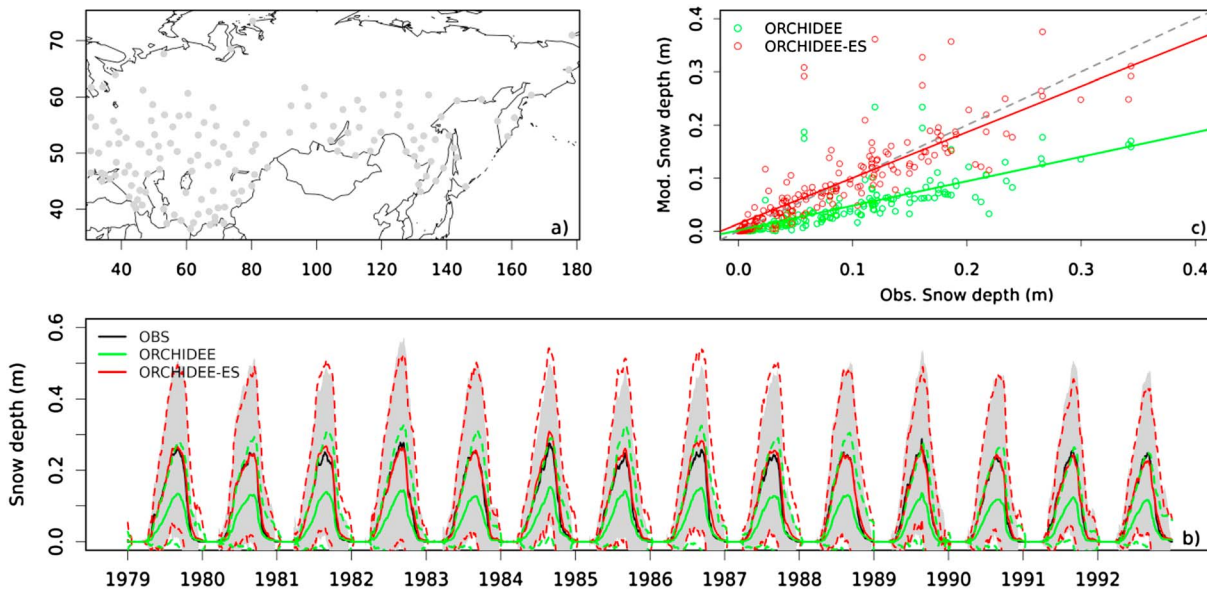


**Figure 10.** (a) Spatial distribution of stations ( $n = 165$ ) having at least 10 years with near complete ( $>360$  days) year-round continuous snow cover; (b) mean daily snow depth comparison between observation and simulations across stations over the period 1979–1992. The gray region represents  $\pm 1$  standard deviation of mean daily observation. The dashed blue (or red) line represents  $\pm 1$  standard deviation of mean daily ORCHIDEE (or ORCHIDEE-ES) values; (c) the scatter plot of multiyear averaged (1979–1992) annual snow depth between observation and simulations across stations.

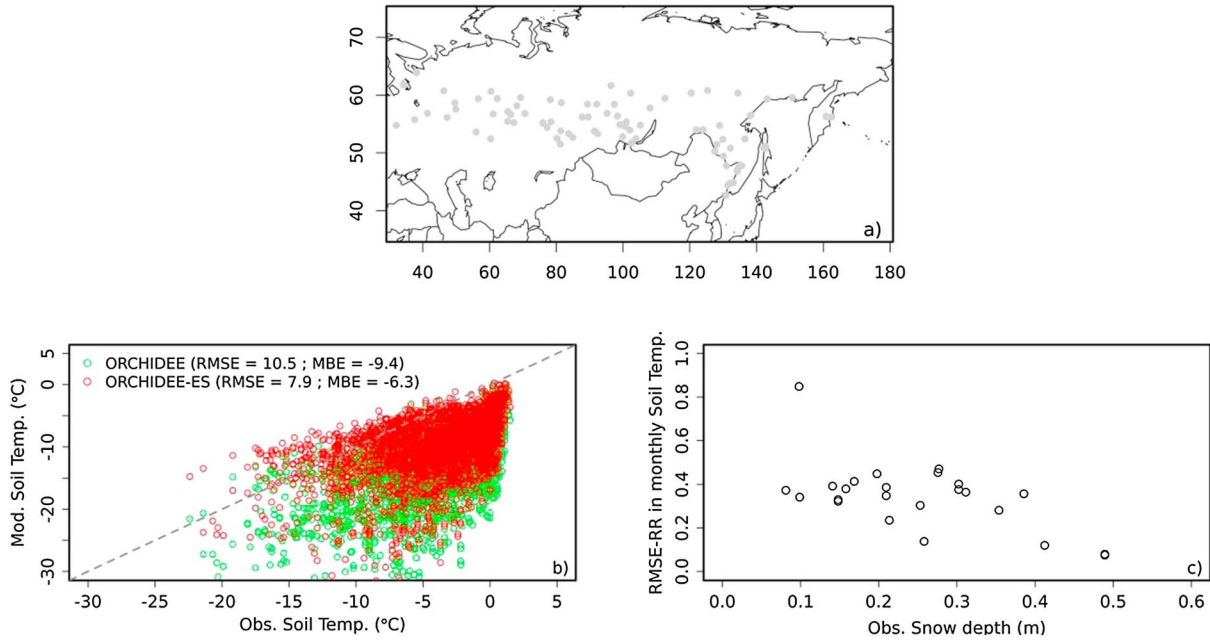


**Figure 11.** (a) Spatial distribution of stations having monthly soil temperature; (b) the scatter plot of monthly soil temperature between observation and simulations from all winter months, years and stations; (c) the relationship between RMSE-RR (see equation (20)) in monthly soil temperature and multiyear averaged monthly snow depth across stations. The stations having at least 10 years of monthly soil temperature are included in this analysis. The month here is only referenced to the winter month (December throughout February).

evidence of the importance of snow thermal conductivity parameterizations. It is interesting to note that the RMSE reduction decreases as mean snow depth increases across sites (Figure 11c), suggesting that the relative advantage of ORCHIDEE-ES over ORCHIDEE in the simulation of 20 cm soil temperature gets reduced if a site was covered by deep snowpack. This implies that the benefits of a physical snow model could be more important for soil temperature simulations at shallow snow regions (or conditions) experiencing, e.g., continued global warming [IPCC, 2007]. In other words, the sensitivity of the surface temperature to snow pack could be higher for shallow snow depth.

[46] The ORCHIDEE-ES cold bias is reduced but not eliminated by the use of the improved snow model (Figure 11b). We therefore suspect that part of the bias could originate from other causes. Firstly, it relates to the possibility that soil freezing processes are not considered in ORCHIDEE-ES. The latent heat released by soil freezing in the autumn or early winter delays the soil cooling [Boike, et al., 1998]. This freezing-induced heat release might endure over the winter if the uppermost soil is effectively insulated by the snow cover. Based on ORCHIDEE, Gouttevin et al. [2012b] showed that the cold bias in soil temperature simulations have been partly removed after adding the soil freezing processes. Moreover, they pointed out that the remained cold biases in soil temperature simulations were ascribed to the deficient snow representation in ORCHIDEE using default snow scheme. In addition, soil thermal insulation by soil carbon can also contribute to the cold bias [Koven et al., 2009]. Thus, future studies can further investigate this issue based on ORCHIDEE-ES including soil freezing/thawing processes [Gouttevin et al., 2012b] and soil thermal insulation

by soil carbon [Koven et al., 2009] developed independently. However, we should inform that this study is not designed for fully bridging the gap in soil temperature simulations but more for understanding the contributing effect of improved snow physics to soil temperature simulations in high-latitude regions.

## 6. Summary and Outlook

[47] The mechanistic intermediate complexity snow scheme ISBA-ES has been adapted and implemented into ORCHIDEE LSM. This three-layered snow module adds more features (e.g., varying snow density and snow thermal conductivity, thawing and refreezing of liquid water within the snowpack) into the original one to simulate the snow processes more accurately. The improved snow scheme shows remarkable performances on snow depth and snow water equivalent simulations over CDP and the sites spanning a large spatial and temporal pattern in northern Eurasia. The enhancements can also be found in daily runoff simulations. As exemplified using CDP data, the snow albedo is shown to be a main determinant for model discrepancy in simulations of main snow variables. This possibly opens new perspectives to improve snow model behaviors in the future through nudging the time evolution of snow albedo from satellite images into ORCHIDEE. But soil temperature simulation cannot truly be benefited if only snow albedo is better modeled. This justifies the necessity of discarding constant snow thermal conductivity but introducing a parameterized one using varying snow density and other factors (e.g., snow temperature and vapor transfer) in the improved snow scheme. ORCHIDEE-ES can then be

adopted to investigate how soil carbon stocks respond to spatio-temporal change of snow thermal conductivity.

[48] We also perform a parameter sensitivity analysis on ORCHIDEE-ES in order to assess the relative importance of physical snow processes influencing snow accumulation/melt and soil temperature. The Morris method used for parameter ranking highlights the processes that should be better characterized (such as wet snow metamorphism, snow compaction rate) in order to constrain model uncertainties.

[49] Finally, the present study focuses only on snow simulation over short vegetation or bare ground. The snow processes in forested areas present different features that cannot easily be implemented into a single-layer energy budget model like ORCHIDEE, since separate layers are needed to resolve energy exchanges between above canopy and atmosphere and between under-canopy atmosphere and snow surface [Harding and Pomeroy, 1996; Link and Marks, 1999; Ellis et al., 2010]. A multilayer representation of the energy balance (under development in the ORCHIDEE team, J. Ryder, personal communication) combined with the multilayer snow scheme presently under development will permit us in the near future to better explore impacts of snow on climate, carbon, and hydrological cycling in a coupled atmosphere-land/snow model.

### Appendix A: Morris Global Sensitivity Analysis Method

[50] In order to assess the influence of parameters, a common method is the analysis of the influence of the parameters on model output one by one. However, this method does not take into account interactions between model parameters [e.g., Saltelli et al., 2008; Campolongo et al., 2011]. Global sensitivity analysis aims to fill this gap by considering entire model parameter space as well as parameter interactions. The method used in this work is the Morris method that consists in randomly choosing a series of parameter combinations that best represent the model parameter space (see details in Morris [1991]; Campolongo et al. [2007]).

[51] In a randomly selected parameter space (or trajectory), the Morris method consists of repetitions of sensitivity

analysis whereby the derivatives are calculated for each parameter  $P_i$  by adding a small change ( $\Delta$ ). The change in model output  $Y(\dots, P_i + \Delta, \dots)$  can then be attributed to such a modification by means of an elementary effect,  $ee_i(Y)$  defined by equation (A1).

$$ee_i(Y) = \frac{Y(\dots, P_i + \Delta, \dots) - Y(\dots, P_i, \dots)}{\Delta} \quad (A1)$$

[52] Where  $\Delta$  is a predefined perturbation factor of  $P_i$ . Each input parameter,  $P_i$ , can only take values corresponding to (a predefined set of evenly spaced)  $p$  levels within its range. The calculation of these elementary effects,  $ee_i(Y)$ , is performed in  $r$  trajectories. The Morris method design only requires  $r*(k+1)$  model simulations to determine a  $ee_i(Y)$  for each of the total  $k$  parameters.

[53] Sensitivity indices  $\mu^*$  from  $ee_i(Y)$  (the average of elementary effects' absolute values) is adopted to rank the parameters according to their influence on the modeled variable. The value of  $\mu^*$  provides information about the importance of each parameter; the larger the value of  $\mu^*$ , the more important the parameter, which defines a ranking for multiple parameters. The Morris method provides qualitative sensitivity analysis measures that allow ranking the parameters in order of importance but do not quantify exactly the relative importance of the parameters.

[54] In this study, we chose 20 parameters that are related to snow simulations in ORCHIDEE-ES. Among them, five parameters related to snow albedo, one to snow roughness length, five to snow thermal properties, three to snow water holding capacity, and six to snow compaction (Table A1). The selection of value ranges for each parameter is of importance because it can impact the results of Morris global sensitivity analysis. The parameter ranges are based on literature survey and expert opinions. If both are not available, the input parameter uncertainty is fixed at 50% of the default value. Here the target variables used to rank the parameters are the root mean square error (RMSE) of snow depth, SWE, and soil temperature at the depth of 10 cm (equation (A1)). The Morris settings of the parameter space (the number of levels,  $p$ , and the number of trajectories,  $r$ ) are left to the user choice. In our analysis, the Morris global sensitivity analysis is carried out for CDP site with Morris settings of  $p=8$  and  $r=40$ , therefore requiring 840 model runs.

**Table A1.** Characteristics of the 20 Selected Model Parameters and Their Associated Default Value and Value Ranges for the Morris Method

Parameter Abbreviation	Parameter Description (Units)	Default Value	Value Ranges
<i>Snow albedo</i>			
$\alpha_{max}$	Maximum snow albedo (-)	0.85	0.70 ~ 1.0
$\alpha_{min}$	Minimum snow albedo (-)	0.50	0.30 ~ 0.60
$\tau_f$	Wet snow albedo decay rate (s)	0.24	0.12 ~ 0.36
$\tau_a$	Dry snow albedo decay rate (s)	0.008	0.004 ~ 0.012
$W_{crm}$	Snow amount for refresh (mm)	10	5 ~ 15
Snow roughness			
$Z_{0n}$	Snow surface roughness length (mm)	1	0.1 ~ 10
<i>Snow thermal properties</i>			
$a_\lambda$	Snow thermal conductivity parameter ( $W m^{-1}$ )	0.02	0 ~ 0.10
$b_\lambda$	Snow thermal conductivity parameter ( $W m^5 K^{-1} kg^{-2}$ )	$2.5 \times 10^{-6}$	$1.0 \times 10^{-7} \sim 5.0 \times 10^{-6}$
$a_{\lambda v}$	Snow thermal conductivity (vapor) parameter ( $W m^{-1} K^{-1}$ )	-0.06	-0.09 ~ -0.03
$b_{\lambda v}$	Snow thermal conductivity (vapor) parameter ( $W m^{-1}$ )	-2.54	-3.81 ~ -1.27
$c_{\lambda v}$	Snow thermal conductivity (vapor) parameter (K)	-289.99	-300.0 ~ -280.0
Liquid water			
$r_{w_{min}}$	Maximum snow liquid water content parameter (-)	0.03	0.015 ~ 0.045

**Table A1.** (continued)

Parameter Abbreviation	Parameter Description (Units)	Default Value	Value Ranges
$rW_{\max}$	Maximum snow liquid water content parameter (–)	0.10	0.05 ~ 0.15
$\rho_z$	Maximum snow liquid water content parameter ( $\text{kg m}^{-3}$ )	200	100 ~ 300
<i>Snow compaction</i>			
$a_{sc}$	Snow settling parameter ( $\text{s}^{-1}$ )	$2.8 \times 10^{-6}$	$1.4 \times 10^{-6} \sim 4.2 \times 10^{-6}$
$b_{sc}$	Snow settling parameter ( $\text{K}^{-1}$ )	0.042	0.02 ~ 0.06
$c_{sc}$	Snow settling parameter ( $\text{m}^3 \text{kg}^{-1}$ )	460	230 ~ 690
$a_{\eta}$	Snow Newtonian viscosity parameter ( $\text{K}^{-1}$ )	0.081	0.0405 ~ 0.12
$b_{\eta}$	Snow Newtonian viscosity parameter ( $\text{m}^3 \text{kg}^{-1}$ )	0.018	0.009 ~ 0.027
$\eta_0$	Snow Newtonian viscosity parameter (Pa s)	$3.7 \times 10^7$	$1.85 \times 10^7 \sim 5.55 \times 10^7$

[56] **Acknowledgments.** The authors are thankful to the Institute of Geography, Russian Academy of Sciences (Moscow, Russia), the State Hydrometeorological Service (Obninsk, Russia), and NSIDC (Boulder, USA) which collected, processed, or delivered the snow observation data used in the present study. We are also thankful to the numerous observers from the Former Soviet Union who performed these precious observations under very harsh meteorological conditions. We would also acknowledge both PhD funding from Commissariat à l’Energie Atomique et aux Energies Alternatives (CEA) in France and post-doc funding by the French national ANR program (CLASSIQUE) and PAGE21 projects.

## References

- Anderson, E. A. (1976), A Point Energy and Mass Balance Model of a Snow Cover, NOAA Technical Report NWS 19, pp 150.
- Armstrong, R. L. (2001), *Historical Soviet Daily Snow Depth Version 2 (HSDSD)/CD-ROM*. National Snow and Ice Data Center, Boulder, Colorado.
- Baker, D. G., D. L. Ruschy, and D. B. Wall (1990), The albedo decay of Prairie snows, *J. Appl. Meteorol.*, 29(2), 179–187.
- Boike, J., K. Roth, and P. P. Overduin (1998), Thermal and hydrologic dynamics of the active layer at a continuous permafrost site (Taymyr Peninsula, Siberia), *Water Resour. Res.*, 34(3), 355–363, doi:10.1029/97WR03498.
- Boone, A., and P. Etchevers (2001), An intercomparison of three snow schemes of varying complexity coupled to the same land surface model: Local-scale evaluation at an Alpine site, *J. Hydrometeorol.*, 2(4), 374–394.
- Brown, R., P. Bartlett, M. MacKay, and D. Verseghy (2006), Evaluation of snow cover in CLASS for SnowMIP, *Atmos.-Ocean*, 44(3), 223–238, doi:10.3137/ao.440302.
- Brun, E., E. Martin, V. Simon, C. Gendre, and C. Coleou (1989), An energy and mass model of snow cover suitable for operational avalanche forecasting, *J. Glaciol.*, 35, 333–342.
- Brun, E., P. David, M. Sudul, and G. Brunot (1992), A numerical-model to simulate snow-cover stratigraphy for operational avalanche forecasting, *J. Glaciol.*, 38(128), 13–22.
- Brun, E., V. Vionnet, A. Boone, B. Decharme, Y. Peings, R. Valette, F. Karbou and S. Morin (2013), Simulation of northern Eurasian local snow depth, mass and density using a detailed snowpack model and meteorological reanalyses, *J. Hydrometeorol.*, 14, 203–219, doi:10.1175/JHM-D-12-012.1.
- Calonne, N., F. Flin, S. Morin, B. Lesaffre, S. Rolland du Roscoat and C. Geindreau (2011), Numerical and experimental investigations of the effective thermal conductivity of snow, *Geophys. Res. Lett.*, 38, L23501, doi:10.1029/2011GL049234.
- Campolongo, F., J. Cariboni, and A. Saltelli (2007), An effective screening design for sensitivity analysis of large models, *Environ. Model. Software*, 22(10), 1509–1518.
- Campolongo, F., A. Saltelli, and J. Cariboni (2011), From screening to quantitative sensitivity analysis. A unified approach, *Comput. Phys. Commun.*, 182(4), 978–988, doi:10.1016/j.cpc.2010.12.039.
- Chalita, S., and H. Le Treut (1994), The albedo of temperate and boreal forest and the northern-hemisphere climate—A sensitivity experiment using the LMD-GCM, *Climate Dynamics*, 10(4–5), 231–240.
- Dee, D. P., et al. (2011), The ERA-Interim reanalysis: Configuration and performance of the data assimilation system, *Q. J. R. Meteorolog. Soc.*, 137(656), 553–597, doi:10.1002/qj.828.
- Douville, H. (2010), Relative contribution of soil moisture and snow mass to seasonal climate predictability: A pilot study, *Climate Dynamics*, 34(6), 797–818, doi:10.1007/s00382-008-0508-1.
- Durand, Y., E. Brun, L. Mérindol, G. Guyomarc’h, B. Lesaffre, and E. Martin (1993), A meteorological estimation of relevant parameters for snow models, *Ann. Glaciol.*, 18, 65–71.
- Dutra, E., P. Viterbo, P. M. A. Miranda, and G. Balsamo (2012), Complexity of snow schemes in a climate model and its impact on surface energy and hydrology, *J. Hydrometeorol.*, 13(2), 521–538, doi:10.1175/jhm-d-11-072.1.
- Dyer, J. L., and T. L. Mote (2006), Spatial variability and trends in observed snow depth over North America, *Geophys. Res. Lett.*, 33(16), doi:10.1029/2006GL027258.
- Ellis, C. R., J. W. Pomeroy, T. Brown, and J. MacDonald (2010), Simulation of snow accumulation and melt in needleleaf forest environments, *Hydrol. Earth Syst. Sci.*, 14(6), 925–940, doi:10.5194/hess-14-925-2010.
- Essery, R., and P. Etchevers (2004), Parameter sensitivity in simulations of snowmelt, *J. Geophys. Res.-Atmos.*, 109(D20), doi:10.1029/2004JD005036.
- Essery, R., E. Martin, H. Douville, A. Fernandez, and E. Brun (1999), A comparison of four snow models using observations from an alpine site, *Climate Dynamics*, 15(8), 583–593, doi:10.1007/s003820050302.
- Essery, R., S. Morin, Y. Lejeune, C. B. Ménard (2013), A comparison of 1701 snow models using observations from an alpine site, *Adv. Water Resour.*, 55, 131–148, doi:10.1016/j.advwatres.2012.07.013.
- Etchevers, P., et al. (2004), Validation of the energy budget of an alpine snowpack simulated by several snow models (SnowMIP project), *Annals of Glaciology*, 38(1), 150–158.
- Fernandes, R., H. X. Zhao, X. J. Wang, J. Key, X. Qu, and A. Hall (2009), Controls on Northern Hemisphere snow albedo feedback quantified using satellite Earth observations, *Geophys. Res. Lett.*, 36, L21702, doi:10.1029/2009GL040057.
- Flanner, M. G., K. M. Shell, M. Barlage, D. K. Perovich, and M. A. Tschudi (2011), Radiative forcing and albedo feedback from the Northern Hemisphere cryosphere between 1979 and 2008, *Nat. Geosci.*, 4(3), 151–155, doi:10.1038/ngeo1062.
- Fletcher, C. G., P. J. Kushner, A. Hall, and X. Qu (2009), Circulation responses to snow albedo feedback in climate change, *Geophys. Res. Lett.*, 36, L09702, doi:10.1029/2009GL038011.
- Gong, G., J. Cohen, D. Entekhabi, and Y. Ge (2007), Hemispheric-scale climate response to Northern Eurasia land surface characteristics and snow anomalies, *Global Planet. Change*, 56(3–4), 359–370, doi:10.1016/j.gloplacha.2006.07.025.
- Gouttevin, I., M. Menegoz, F. Domine, G. Krinner, C. Koven, P. Ciais, C. Tarnocai, and J. Boike (2012a), How the insulating properties of snow affect soil carbon distribution in the continental pan-Arctic area, *J. Geophys. Res.-Biogeosci.*, 117, doi:10.1029/2011JG001916.
- Gouttevin, I., G. Krinner, P. Ciais, J. Polcher, and C. Legout (2012b), Multi-scale validation of a new soil freezing scheme for a land-surface model with physically-based hydrology, *Cryosphere*, 6(2), 407–430, doi:10.5194/tc-6-407-2012.
- Groisman, P. Y., T. R. Karl, R. W. Knight, and G. L. Stenchikov (1994), Changes of snow cover, temperature, and radiative heat-balance over the Northern Hemisphere, *J. Climate*, 7(11), 1633–1656.
- Groisman, P. Y., R. W. Knight, T. R. Karl, D. R. Easterling, B. M. Sun, and J. H. Lawrimore (2004), Contemporary changes of the hydrological cycle over the contiguous United States: Trends derived from in situ observations, *J. Hydrometeorol.*, 5(1), 64–85.
- Habets, F., et al. (2008), The SAFRAN-ISBA-MODCOU hydrometeorological model applied over France, *J. Geophys. Res.-Atmos.*, 113(D6), doi:10.1029/2007JD008548.
- Harding, R. J., and J. W. Pomeroy (1996), Energy balance of the winter boreal landscape, *J. Climate*, 9(11), 2778–2787.
- Hock, R. (2003), Temperature index melt modelling in mountain areas, *J. Hydrol.*, 282(1–4), 104–115, doi:10.1016/s0022-1694(03)00257-9.
- Intergovernmental Panel on Climate Change (IPCC) (2007), *Climate Change 2007: The Scientific Basis. Contribution of Working Group I to*

- the *Fourth Assessment Report of the Intergovernmental Panel on Climate Change*, edited by S. Solomon et al., Cambridge Univ. Press, New York.
- Kodama, M., K. Nakai, S. Kawasaki, and M. Wada (1979), An application of cosmic-ray neutron measurements to the determination of the snow-water equivalent, *J. Hydrol.*, *41*, 85–92, doi:10.1016/0022-1694(79)90107-0.
- Kojima, K. (1967), Densification of a seasonal snow cover, *Physics of Snow and Ice: Proceedings International Conference on Low Temperature Science*, *1*(2), 929–952.
- Koven, C., P. Friedlingstein, P. Ciais, D. Khvorostyanov, G. Krinner, and C. Tamocai (2009), On the formation of high-latitude soil carbon stocks: Effects of cryoturbation and insulation by organic matter in a land surface model, *Geophys. Res. Lett.*, *36*, L21501, doi:10.1029/2009GL040150.
- Krenke, A. (2004), Former Soviet Union hydrological snow surveys, 1966–1996. *National Snow and Ice Data Center/World Data Center for Glaciology*, Boulder.
- Kuipers Munneke, P., M. R. van den Broeke, J. T. M. Lenaerts, M. G. Flanner, A. S. Gardner, and W. J. van de Berg (2011), A new albedo parameterization for use in climate models over the Antarctic ice sheet, *J. Geophys. Res.*, *116*, D05114, doi:10.1029/2010JD015113.
- Lehning M., P. B. Bartelt, R. L. Brown, C. Fierz, and P. Satyawali (2002), A physical SNOWPACK model for the Swiss Avalanche Warning Services. *Part II: Snow Microstructure, Cold Regions Science and Technology*, *35*, 147–167.
- Lemke, P., et al. (2007), Observations: Changes in Snow, Ice and Frozen Ground. In: *Climate Change 2007: The Physical Science Basis. Contribution of Working Group I to the Fourth Assessment Report of the Intergovernmental Panel on Climate Change* [Solomon, S., D. Qin, M. Manning, Z. Chen, M. Marquis, K.B. Averyt, M. Tignor and H.L. Miller (eds.)]. Cambridge University Press, Cambridge, United Kingdom and New York, NY, USA.
- Link, T. E., and D. Marks (1999), Point simulation of seasonal snow cover dynamics beneath boreal forest canopies, *J. Geophys. Res.-Atmos.*, *104*(D22), 27841–27857, doi:10.1029/1998JD00121.
- Lynchstieglitz, M. (1994), The development and validation of a simple snow model for the GISS GCM, *J. Climate*, *7*(12), 1842–1855.
- Malik, M. J., R. van der Velde, Z. Vekerdy, and Z. B. Su (2012), Assimilation of satellite-observed snow albedo in a land surface model, *J. Hydrometeorol.*, *13*(3), 1119–1130, doi:10.1175/jhm-d-11-0125.1.
- Martin, E. and Y. Lejeune (1998), Turbulent fluxes above the snow surface, *Annals of Glaciology*, *26*, 179–183.
- Mellor, M. (1964), Properties of snow, *Cold Regions Science and Technology, Monograph III-A1*, pp 105.
- Morin, S., Y. Lejeune, B. Lesaffre, J. M. Panel, D. Poncet, P. David, and M. Sudul (2012), A 18-yr long (1993–2011) snow and meteorological dataset from a mid-altitude mountain site (Col de Porte, France, 1325 m alt.) for driving and evaluating snowpack models. *Earth System Science Data*, *4*(1), 13–21, doi:10.5194/essd-4-13-2012.
- Morris, M. D. (1991), Factorial sampling plans for preliminary computational experiments, *Technometrics*, *33*(2), 161–174.
- Noilhan, J., and P. Lacarrere (1995), GCM grid-scale evaporation from mesoscale modeling, *J. Climate*, *8*(2), 206–223.
- Pan, M., et al. (2003), Snow process modeling in the North American Land Data Assimilation System (NLDA): 2. Evaluation of model simulated snow water equivalent, *J. Geophys. Res.-Atmos.*, *108*(D22), 8850, doi:10.1029/2003JD003994.
- Paquet, E., and M. T. Laval (2006), Operation feedback and prospects of EDF Cosmic-Ray Snow Sensors, *La Houille Blanche*, *2*, 113–119, doi:10.1051/lhb:200602015.
- Parajka, J., S. Dadson, T. Lafon, and R. Essery (2010), Evaluation of snow cover and depth simulated by a land surface model using detailed regional snow observations from Austria, *J. Geophys. Res.-Atmos.*, *115*, D24117, doi:10.1029/2010JD014086.
- Peng, S. S., S. L. Piao, P. Ciais, J. Y. Fang, and X. H. Wang (2010), Change in winter snow depth and its impacts on vegetation in China, *Glob. Chang. Biol.*, *16*(11), 3004–3013, doi:10.1111/j.1365-2486.2010.02210.X.
- Piao, S. L., P. Friedlingstein, P. Ciais, N. de Noblet-Ducoudre, D. Labat, and S. Zaehle (2007), Changes in climate and land use have a larger direct impact than rising CO<sub>2</sub> on global river runoff trends, *Proc. Natl. Acad. Sci. U.S.A.*, *104*(39), 15242–15247, doi:10.1073/pnas.0707213104.
- Polcher, J., et al. (1998), A proposal for a general interface between land surface schemes and general circulation models, *Global Planet. Change*, *19*(1–4), 261–276, doi:10.1016/s0921-8181(98)00052-6.
- Qu, X., and A. Hall (2006), Assessing snow albedo feedback in simulated climate change, *J. Climate*, *19*(11), 2617–2630, doi:10.1175/jcli3750.1.
- Rasmus, S., T. Gronholm, M. Lehning, K. Rasmus, and M. Kulmala (2007), Validation of the SNOWPACK model in five different snow zones in Finland, *Boreal Environ. Res.*, *12*(4), 467–488.
- Robinson, D. A., K. F. Dewey, and R. R. Heim (1993), Global snow cover monitoring—An update, *Bull. Am. Meteorol. Soc.*, *74*(9).
- Rutter, N., et al. (2009), Evaluation of forest snow processes models (SnowMIP2), *J. Geophys. Res.-Atmos.*, *114*, D06111, doi:10.1029/2008JD011063.
- Saltelli, A., M. Ratto, T. Andres, F. Campolongo, J. Carboni, D. Gatelli, M. Saisana, and S. Tarantola (2008), *Global Sensitivity Analysis. The Primer*, John Wiley & Sons Ltd, Chichester, England.
- Shrestha, M., L. Wang, T. Koike, Y. Xue, and Y. Hirabayashi (2010), Improving the snow physics of WEB-DHM and its point evaluation at the SnowMIP sites, *Hydrol. Earth Syst. Sci.*, *14*(12), 2577–2594, doi:10.5194/hess-14-2577-2010.
- Slater, A. G., et al. (2001), The representation of snow in land surface schemes: Results from PILPS 2(d), *J. Hydrometeorol.*, *2*(1), 7–25.
- Sturm, M., J. Holmgren, M. König, and K. Morris (1997), The thermal conductivity of seasonal snow, *J. Glaciol.*, *43*(143), 26–41.
- Sun, S. F., J. M. Jin, and Y. K. Xue (1999), A simple snow-atmosphere-soil transfer model, *J. Geophys. Res.-Atmos.*, *104*(D16), 19587–19597, doi:10.1029/1999JD900305.
- Tahir, A. A., P. Chevallier, Y. Arnaud, and B. Ahmad (2011), Snow cover dynamics and hydrological regime of the Hunza River basin, Karakoram Range, Northern Pakistan, *Hydrol. Earth Syst. Sci.*, *15*(7), 2275–2290, doi:10.5194/hess-15-2275-2011.
- Verseghy, D. L. (1991), CLASS-A Canadian land surface scheme for GCMs.1. soil model, *Int. J. Climatol.*, *11*(2), 111–133.
- Vionnet, V., E. Brun, S. Morin, A. Boone, S. Faroux, P. Le Moigne, E. Martin, and J. M. Willemet (2012), The detailed snowpack scheme Crocus and its implementation in SURFEX v7.2, *Geoscientific Model Dev.*, *5*(3), 773–791, doi:10.5194/gmd-5-773-2012.
- Yen, Y. C. (1981), Review of the thermal properties of snow, ice and sea ice, *Tech. Rep.*, *81-10*, Cold Regions Research and Engineering Laboratory, Hanover, NH.
- Zhang, T. J., R. Barry, and D. Gilichinsky (2001), *Russian historical soil temperature data, 2001, updated 2006*, *National Snow and Ice Data Center/World Data Center for Glaciology*, Boulder.